# Grouping PMU Signals for Guaranteed Recovery under Corruption: Insights and Recommendations

Kaustav Chatterjee and Nilanjan Ray Chaudhuri
School of Electrical Engineering and Computer Science
The Pennsylvania State University
State College, PA 16801, USA
Email: kuc760@psu.edu; nuc88@psu.edu

George Stefopoulos
Advanced Grid Innovation Lab for Energy
New York Power Authority
White Plains, NY 10601, USA
Email: George.Stefopoulos@nypa.gov

*Abstract*—A connection is established between the system-theoretic notion of modal observability, and the indices guaranteeing robust signal recovery – denseness and restricted isometry. Insights are derived for grouping signals to ensure guaranteed recovery of synchrophasor measurements corrupted with sparse and spurious anomalies. The propositions on signal grouping are validated on simulated data from a IEEE test system, as well as field PMU measurements from a US utility.

*Index Terms*—PMU, Data Recovery, Bad Data, Compressive Sensing, Robust PCA, Denseness, Restricted Isometry.

## I. Introduction

The blackouts in the Western Electricity Coordinating Council (WECC) in July and August 1996, and northeastern United States in August 2003 were pivotal in underscoring the need of wide-area monitoring in large power grids. Since then, major utilities in North America− BPA, PJM, TVA, and NYPA among others, have invested extensively in expanding their network of Phasor Measurement Units (PMUs). PMUs are high fidelity measurement devices capable of reporting GPS-time-synchronised voltage and current measurements across wide geographies at rates much higher than conventional SCADA systems. This has contributed to better visualization of system transients and has enhanced situational awareness, especially in terms of monitoring low frequency electromechanical oscillations [1], [2].

However, the reliability of the algorithms used in monitoring applications is contingent upon the control center receiving error-free PMU measurements. Missing data values, spurious outliers, and corruption from channel noise can compromise the accuracy of these algorithms [3]. Also, as outlined in [4] and [5], a dedicated intranet-based communication network in NASPInet architecture is not immune to cyber attack. These monitoring algorithms therefore, need a data pre-processor to detect and filter out bad data from PMU streams. Ideally, the bad data detection and correction can be done using state estimators at control centers, but this requires full observability of the system with PMUs and an accurate knowledge of system topology. In contrast, considering the present scenario with a limited number of PMUs in most systems, data recovery from grossly corrupted measurements has been achieved by several low-rank matrix completion methods [6]–[10] that exploit spatio-temporal correlation in data streams.

The challenge however is, this requires a careful grouping of signals (vis-à-vis PMU locations) to ensure correlation and low-rankness of the measurement window (i.e. data matrix). To that end, in this paper, we make propositions about grouping candidate signals with similar modal signature. As we shall see later, this translates into higher denseness of the subspace spanned by the measurement window, thereby, enhancing the chances of exact data recovery under corruption.

*Contributions:* In this paper, we draw connections between the signal-theoretic principles of data recovery and system-theoretic notion of modal observability to make propositions on signal selection (or grouping) to guarantee exact data recovery under corruption. We make the following contributions− first, we show that the denseness of a subspace derived from a measurement window can be bounded by denseness of the observability submatrix obtained from the small-signal model corresponding to the poorly-damped modes in the system (under the weak assumption that other modes are sufficiently damped in the window and/or sufficiently unobservable). Second, we derive insights into grouping of signals to enhance the denseness of the observability submatrix to meet the sufficiency condition for guaranteed exact data recovery [11]. Third, we quantify the perturbation in the denseness values for small variations in the magnitudes of modal observabilities within a signal group. And finally, we extend these insights onto recommendations for grouping signals directly from PMU data eliminating the need for a small-signal model.

The remaining paper is organised as follows. In Section II we revisit the sparse optimization-based data recovery approach in [10], and recall the definitions of restricted isometry constant and denseness coefficient, and the sufficiency conditions on these to guarantee sparse recovery following this approach. Next, in Section III we present our contributions described above followed by supporting case studies in Section V. Concluding remarks are summarised in Section VI.

## II. Background

### A. Small-signal Model and Modal Observability

The linearized state-space model of a power system can be described as

$$\dot{\mathbf{x}}(t) = \mathbf{A}\mathbf{x}(t) + \mathbf{B}\mathbf{u}(t), \quad \mathbf{y}(t) = \mathbf{C}\mathbf{x}(t) \qquad (1)$$

where, $\mathbf{x}(t) \in \Re^{m \times 1}$, $\mathbf{y}(t) \in \Re^{n \times 1}$, and $\mathbf{u}(t) \in \Re^{p \times 1}$ are respectively the vectors of state, output, and input variables capturing the perturbations from their respective equilibria.

Assuming $\mathbf{A}$ is diagonalizable, consider the transformation $\mathbf{P}^{-1}\mathbf{x}(t) = \tilde{\mathbf{x}}(t)$ where, $\mathbf{P}$ is the matrix of right eigenvectors of $\mathbf{A}$. The equations in (1) can then be re-written as,

$$\dot{\tilde{\mathbf{x}}}(t) = \mathbf{P}^{-1}\mathbf{A}\mathbf{P}\mathbf{x}(t) + \mathbf{P}^{-1}\mathbf{B}\mathbf{u}(t) = \mathbf{\Lambda}\tilde{\mathbf{x}}(t) + \tilde{\mathbf{B}}\mathbf{u}(t)$$
$$\mathbf{y}(t) = \mathbf{C}\mathbf{P}\tilde{\mathbf{x}}(t) = \mathbf{\Psi}\tilde{\mathbf{x}}(t) \tag{2}$$

where, $\mathbf{\Lambda} \in \Re^{m \times m}$ is the diagonal matrix of the eigenvalues of $\mathbf{A}$. Henceforth, in this paper, we shall refer to each complex-conjugate eigenvalue pair of $\mathbf{\Lambda}$ as a mode, and $\mathbf{\Psi} \in \Re^{n \times m}$ as the matrix of relative modal observabilities [12] mapping the extent to which each mode is visible in the output variables.

### B. Signal Corruption and Robust Recovery

Next, owing to corruption, let the measurements received at the control center be different from $\mathbf{y}(t)$. We model this as

$$\mathbf{z}(t) = \mathbf{y}(t) + \mathbf{e}(t) \tag{3}$$

where, $\mathbf{e}(t)$ is the vector of additive signal corruptions. We assume that the corruptions are limited to only a fraction of all signals, and therefore, $\mathbf{e}(t)$ is a sparse vector with most entries as zeros.

In this paper, we shall use robust principal component analysis (R-PCA)-based anomaly correction approach from [10] for recovering the actual measurements from the corrupted observations $\mathbf{z}(t)$. Building on the theory of compressive sensing [13]–[15], the algorithm in [10] solves a sparse optimization problem to estimate the signal corruption $\hat{\mathbf{e}}(t)$, which can then be subtracted from $\mathbf{z}(t)$ to recover $\hat{\mathbf{y}}(t)$. Henceforth, we shall refer to $\hat{\mathbf{y}}(t)$ as the recovered signal vector at time $t$. The recovery framework is summarised below.

First, define a window $\mathbf{Y}$ of previously recovered samples till the latest instant as shown below,

$$\mathbf{Y} = \begin{bmatrix} \hat{\mathbf{y}}(t - N\tau) & \dots & \hat{\mathbf{y}}(t - \tau) \end{bmatrix} \tag{4}$$

where, $\tau$ is the reporting interval between two successive PMU samples. Then, perform singular value decomposition on $\mathbf{Y}$ to extract the singular vectors corresponding to $r-$dominant singular values, as follows, $\mathbf{Y} = \hat{\mathbf{U}}\hat{\mathbf{\Sigma}}\hat{\mathbf{V}}^H$. Superscript $H$ denotes Hermitian of a matrix.

Next, project $\mathbf{z}(t)$ onto the space orthogonal to the span of $\hat{\mathbf{U}}$ as shown,

$$\boldsymbol{\gamma}(t) = \mathbf{\Phi}\mathbf{z}(t) = \mathbf{\Phi}(\mathbf{y}(t) + \mathbf{e}(t)) = \mathbf{\Phi}\mathbf{e}(t) + \boldsymbol{\nu}(t) \tag{5}$$

where, $\mathbf{\Phi} = \mathbf{I} - \hat{\mathbf{U}}\hat{\mathbf{U}}^H$. Ideally, $\mathbf{y}(t)$ belongs to the span of $\hat{\mathbf{U}}$, and therefore, the projection ensures that the contribution of $\mathbf{y}(t)$ is nullified. However, due to inherent nonlinearities in the signals and because of truncating $\mathbf{Y}$ to $r-$dominant singular values we have a small non-zero term $\boldsymbol{\nu}(t)$ in eqn. (5).

Finally, the estimated corruption vector $\hat{\mathbf{e}}(t)$ is obtained as the solution of the sparse optimization problem below,

$$\min_{\mathbf{e}(\mathbf{t})} \left\|\mathbf{e}(\mathbf{t})\right\|_1 \quad \text{s.t.} \quad \left\|\boldsymbol{\gamma}(t) - \mathbf{\Phi}\mathbf{e}(\mathbf{t})\right\|_2 \leq \eta \tag{6}$$

where $\eta$ is a small thresholding term. The signal can then be recovered as, $\hat{\mathbf{y}}(t) = \mathbf{z}(t) - \hat{\mathbf{e}}(t)$.

### C. Denseness and Guarantees for Exact Signal Recovery

The $l_1-$norm minimization in eqn. (6) is a convex relaxation of the original non-convex $l_0-$norm minimization that maximizes the sparsity of $\hat{\mathbf{e}}(t)$. The $l_0-$norm minimization is NP-hard, the $l_1-$relaxation on the other hand ensures a solution in polynomial time. But the $l_1-$minimization is not always guaranteed to be sparse, implying that, the solution from eqn. (6) may not be an accurate estimate of corruption. It is shown in [13] that a *sufficiency condition* for guaranteeing exact recovery of signals with $s-$sparse corruptions (i.e. ensuring equivalence of $l_0$ and $l_1-$minimizations) is to ensure that the $s-$restricted isometry constant $\delta_s(\mathbf{\Phi})$ is below a desired threshold. Cai et-al in [11] established this threshold to be 0.307, which will be considered in this paper.

One way to interpret the restricted isometry constant $\delta_s(\mathbf{\Phi})$ is in terms of denseness $\kappa_s(\hat{\mathbf{U}})$ of the subspace spanned by the singular vectors in $\hat{\mathbf{U}}$. Denseness coefficient $\kappa_s$ [16] for any matrix $\mathbf{Y}$ is defined as,

$$\kappa_s(\mathbf{Y}) = \kappa_s(\text{range}(\mathbf{Y})) = \max_{|T| \leq s} \left\|(\mathbf{I}_T)^H \text{basis}(\mathbf{Y})\right\|_2 \tag{7}$$

Maximum value that $\kappa_s$ can attain is 1. Lower the value of $\kappa_s$, higher is the denseness of the range space.

As derived in [16], for a basis matrix $\hat{\mathbf{U}}$,

$$\delta_s(\mathbf{\Phi}) = \delta_s(\mathbf{I} - \hat{\mathbf{U}}\hat{\mathbf{U}}^H) = \kappa_s(\hat{\mathbf{U}})^2 \tag{8}$$

Therefore, attaining the sufficiency condition

$$\delta_s(\mathbf{\Phi}) < 0.307 \implies \kappa_s(\mathbf{Y}) = \kappa_s(\hat{\mathbf{U}}) < 0.554 = \kappa^* \tag{9}$$

For different choices of signals− both the size of the set and the individual constituents, the singular vectors spanning $\mathbf{Y}$ would change, and so would the denseness coefficient $\kappa_s(\mathbf{Y})$. Thus motivated, we develop analytical insights on to grouping signals to reduce $\kappa_s(\mathbf{Y})$ below $\kappa^*$, where possible.

## III. Signal Grouping: Insights & Recommendations

**Lemma 1.** $\kappa_s(\mathbf{Y}) \leq \kappa_s(\mathbf{\Psi}) = \max_{|T| \leq s} \left\|(\mathbf{I}_T)^H \mathbf{\Psi}\mathbf{\Psi}^\dagger\right\|_2$

**Proof.** Referring to eqns. (2) and (4),

$$\mathbf{Y} = \mathbf{\Psi} \begin{bmatrix} \tilde{\mathbf{x}}(t - N\tau) & \dots & \tilde{\mathbf{x}}(t - \tau) \end{bmatrix} \triangleq \mathbf{\Psi}\tilde{\mathbf{X}} \tag{10}$$

Therefore, range$(\mathbf{Y}) \subseteq$ range$(\mathbf{\Psi}) \implies \kappa_s(\mathbf{Y}) \leq \kappa_s(\mathbf{\Psi})$. Equality is attained when $\tilde{\mathbf{X}}$ is full row rank.

Next, let $\hat{\mathbf{U}}_{\mathbf{\Psi}}$ be the matrix of singular vectors spanning the range of $\mathbf{\Psi}$. Therefore, following the definition of denseness

$$\kappa_s(\mathbf{\Psi}) = \max_{|T| \leq s} \left\|(\mathbf{I}_T)^H \hat{\mathbf{U}}_{\mathbf{\Psi}}\right\|_2 = \max_{|T| \leq s} \left\|(\mathbf{I}_T)^H \hat{\mathbf{U}}_{\mathbf{\Psi}}\hat{\mathbf{U}}_{\mathbf{\Psi}}^H\right\|_2 \tag{11}$$

Moreover, the range-spaces of $\hat{\mathbf{U}}_{\mathbf{\Psi}}$ and $\mathbf{\Psi}$ being same, the orthogonal projection matrices onto this space can be equated as follows $\hat{\mathbf{U}}_{\mathbf{\Psi}}\hat{\mathbf{U}}_{\mathbf{\Psi}}^H = \mathbf{\Psi}\mathbf{\Psi}^\dagger$, where $\mathbf{\Psi}^\dagger = (\mathbf{\Psi}^H\mathbf{\Psi})^{-1}\mathbf{\Psi}^H$. Substituting this in eqn.(11) we get,

$$\kappa_s(\mathbf{\Psi}) = \max_{|T| \leq s} \left\|(\mathbf{I}_T)^H \hat{\mathbf{U}}_{\mathbf{\Psi}}\hat{\mathbf{U}}_{\mathbf{\Psi}}^H\right\|_2 = \max_{|T| \leq s} \left\|(\mathbf{I}_T)^H \mathbf{\Psi}\mathbf{\Psi}^\dagger\right\|_2 \quad \square$$

*Corollary*: Consider a data window $\mathbf{Y}$ exhibiting oscillatory response due to $k$ poorly-damped modes. Under the weak assumption that the rest of the modes are sufficiently damped and/or sufficiently unobservable in the data window, we can write $\kappa_s(\mathbf{Y}) \leq \kappa_s(\hat{\boldsymbol{\Psi}})$ where, $\hat{\boldsymbol{\Psi}} = \begin{bmatrix} \hat{\boldsymbol{\Psi}}_1 & \hat{\boldsymbol{\Psi}}_2 & \cdots & \hat{\boldsymbol{\Psi}}_k \end{bmatrix}$ is the submatrix of $\boldsymbol{\Psi}$ containing the complex conjugate column-pairs corresponding to the poorly-damped modes of interest, implying each $\hat{\boldsymbol{\Psi}}_j = \begin{bmatrix} \boldsymbol{\psi}_j & \overline{\boldsymbol{\psi}}_j \end{bmatrix}$ for $j = 1, 2, \ldots, k$.

It can be shown that, for a $r-$rank $\hat{\boldsymbol{\Psi}}$, the minimum value that $\kappa_1(\hat{\boldsymbol{\Psi}})$ can achieve is $\sqrt{\frac{r}{n}}$. Therefore, the minimum value of $\kappa_1(\hat{\boldsymbol{\Psi}})$ is achieved when signals are selected in way such that corresponding $\hat{\boldsymbol{\Psi}}$ has rank 1. To that end, we present lemmas 2 and 3 for a unimodal case.

**Lemma 2.** For a unimodal case, if the complex entries in $\boldsymbol{\psi}_1$ have same phase angle then, rank($\hat{\boldsymbol{\Psi}}$) is 1.

**Proof.** Let $\boldsymbol{\psi}_1 = \begin{bmatrix} |\psi_{11}|\underline{/\theta} & \cdots & |\psi_{1i}|\underline{/\theta} & \cdots & |\psi_{1n}|\underline{/\theta} \end{bmatrix}^T$ and therefore, $\overline{\boldsymbol{\psi}}_1 = \begin{bmatrix} |\psi_{11}|\underline{/-\theta} & \cdots & |\psi_{1i}|\underline{/-\theta} & \cdots & |\psi_{1n}|\underline{/-\theta} \end{bmatrix}^T$.

Next, we perform Gram-Schmidt orthonormalization to find the bases spanning the columns of $\hat{\boldsymbol{\Psi}}_1$. Let the orthonormal bases be $\hat{\mathbf{u}}_1$ and $\hat{\mathbf{u}}_2$, such that, $\hat{\mathbf{u}}_1 = \frac{\mathbf{u}_1}{\|\mathbf{u}_1\|_2} = \frac{\boldsymbol{\psi}_1}{\|\boldsymbol{\psi}_1\|_2}$, and $\hat{\mathbf{u}}_2 = \frac{\mathbf{u}_2}{\|\mathbf{u}_2\|_2}$ where, $\mathbf{u}_2 = \overline{\boldsymbol{\psi}}_1 - \frac{\langle \boldsymbol{\psi}_1, \overline{\boldsymbol{\psi}}_1 \rangle}{\langle \boldsymbol{\psi}_1, \boldsymbol{\psi}_1 \rangle} \boldsymbol{\psi}_1$. Since $\langle \boldsymbol{\psi}_1, \overline{\boldsymbol{\psi}}_1 \rangle = \|\boldsymbol{\psi}_1\|_2^2 \underline{/-2\theta}$, we can express any $i^{\text{th}}$ entry of $\mathbf{u}_2$ as,

$$u_{2i} = |\psi_{1i}|\underline{/-\theta} - \frac{\|\boldsymbol{\psi}_1\|_2^2 \underline{/-2\theta}}{\|\boldsymbol{\psi}_1\|_2^2} |\psi_{1i}|\underline{/\theta} = 0 \quad (12)$$

This implies $\hat{\mathbf{u}}_2 = \mathbf{0}$, and therefore, rank($\hat{\boldsymbol{\Psi}}$) is 1. $\square$

*Corollary*: The rank 1 property ensures that $\kappa_1(\hat{\boldsymbol{\Psi}}) = \kappa_1(\boldsymbol{\psi}_1)$. This simplifies the problem as the analysis now reduces to calculating the denseness of a column vector.

**Lemma 3.** For a unimodal case, the minimum value of $\kappa_1(\hat{\boldsymbol{\Psi}})$ is attained when signals are selected from a coherent group with minimum variance in the magnitudes of relative modal observabilities.

**Proof.** Signals selected from a single coherent group oscillate in unison, and hence, it can be inferred that their modal observabilities have same phase. Therefore, following Lemma 2, rank($\hat{\boldsymbol{\Psi}}$) is 1.

Next, let $\{\mathbf{e}_1, \ldots \mathbf{e}_i, \ldots \mathbf{e}_n\}$ be the set of standard basis vectors. The denseness $\kappa_1$ can then be calculated as,

$$\kappa_1(\hat{\boldsymbol{\Psi}}) = \max_i \left\| \mathbf{e}_i^H \text{basis}(\hat{\boldsymbol{\Psi}}) \right\|_2 = \max_i \left\| \mathbf{e}_i^H \hat{\mathbf{u}}_1 \right\|_2 = \|\hat{\mathbf{u}}_1\|_\infty$$
$$= \frac{\|\boldsymbol{\psi}_1\|_\infty}{\|\boldsymbol{\psi}_1\|_2} = \frac{|\psi_{1i}|_{max}}{\sqrt{\sum_{i=1}^n |\psi_{1i}|^2}} \geq \frac{1}{\sqrt{n}} \quad (13)$$

The minimum value $\frac{1}{\sqrt{n}}$ is attained when $|\psi_{1i}|$ s are equal. $\square$

However, this being too ideal a scenario, we next investigate how the denseness coefficient $\kappa_1$ changes with variation in the magnitudes of modal observabilities, especially in for of an large magnitude outlier in the observability vector.

For this, we divide the signal set into two groups− (1) the signal with index $i_{max}$ having the highest magnitude of observability $|\psi_{1i}|_{max}$, and (2) the remaining $n-1$ signals with observability magnitudes $|\psi_{1i}|$-s dispersed with mean $\mu$ and standard deviation $\sigma$. Since $|\psi_{1i}|_{max} \geq |\psi_{1i}| \; \forall \; i$, it can be expressed as $|\psi_{1i}|_{max} = \mu + \rho\sigma$ for some $\rho \geq 1$. The parameter $\rho$ controls the extent to which the signal with the highest observability magnitude deviates from the remaining.

Therefore, $\sum_{i=1}^n |\psi_{1i}|^2 = |\psi_{1i}|_{max}^2 + \sum_{i=1, \; i \neq i_{max}}^n |\psi_{1i}|^2$
$$= (\mu + \rho\sigma)^2 + (n-1)(\mu^2 + \sigma^2) \quad (14)$$

Substituting this in (13), $\kappa_1(\hat{\boldsymbol{\Psi}}) = \dfrac{1}{\sqrt{1 + \frac{(n-1)(\mu^2 + \sigma^2)}{(\mu + \rho\sigma)^2}}}$ (15)

Eqn. (15) shows that $\kappa_1(\hat{\boldsymbol{\Psi}})$ is a decreasing function of $n$, and an increasing function of $\rho$. Therefore, a signal with very large $|\psi_{1i}|$ compared to the rest (i.e. large $\rho$), although attractive for oscillation monitoring, might increase $\kappa_1(\hat{\boldsymbol{\Psi}})$ undesirably.

*Recommendations:* Based on Lemmas $1-3$, for a dominantly unimodal scenario, the following recommendations for signal grouping are made to ensure $\kappa_1(\mathbf{Y}) < \kappa^*$ : (a) variation in magnitudes and angles of modal observabilities should be minimized, (b) large outliers with high observability should be avoided, and (c) while adhering to (a) and (b), the number of signals in the group should be increased where possible. $\square$

Next, considering the recommendations above, let signals be grouped with variance in $|\psi_{1i}|$ minimized, such that we can assume $\frac{\mu}{\sigma} >> 1$ and $\rho$ in the neighborhood of 1. Under these conditions, we can approximate eqn. (15) as follows.

$$\kappa_1(\hat{\boldsymbol{\Psi}}) = \kappa_1(\boldsymbol{\psi}_1) = \frac{\rho + \frac{\mu}{\sigma}}{\sqrt{(\rho + \frac{\mu}{\sigma})^2 + (n-1)(1 + \frac{\mu^2}{\sigma^2})}}$$
$$\approx \frac{\rho + \frac{\mu}{\sigma}}{\sqrt{n}\frac{\mu}{\sigma}} = \frac{1}{\sqrt{n}}\left(1 + \frac{\rho\sigma}{\mu}\right) \quad (16)$$

Eqn. (16) shows that for sets sufficiently dense, $\kappa_1$ increases linearly with $\rho$ and $\sigma$ from its minimum (and ideal) value $\frac{1}{\sqrt{n}}$.

*Remarks:* Building on the notion that a signal with multiple modes can be decomposed into its constituent frequencies, the recommendations above can be extended for enhancing denseness for each mode, to ensure overall signal denseness.

## IV. CASE STUDIES

### A. Case I: Grouping Signals based on Small-Signal Model

We consider Kundur's $2-$area $4-$machine system [12] with slight modification as shown in Fig 1. The system exhibits a poorly-damped 0.63-Hz inter-area mode under nominal condition. In this study, we consider two groups of voltage angle signals, with their relative modal observabilities listed in Tables I and II.
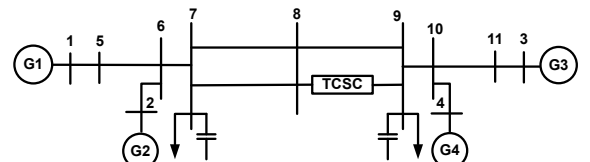


Fig. 1: $2-$area $4-$machine test system with TCSC

TABLE I: SIGNALS AND RELATIVE MODAL OBSERVABILITIES

| signals | $\theta_1 - \theta_3$ | $\theta_4 - \theta_3$ | $\theta_{10} - \theta_3$ | $\theta_{11} - \theta_3$ |
|---|---|---|---|---|
| $\lvert\psi_{1i}\rvert$ | 9.462 | 1.085 | 1.611 | 0.635 |
| $\angle\psi_{1i}$ | $\angle-84.32°$ | $\angle-84.16°$ | $\angle-84.26°$ | $\angle-84.18°$ |

TABLE II: SIGNALS AND RELATIVE MODAL OBSERVABILITIES

| signals | $\theta_1 - \theta_3$ | $\theta_2 - \theta_3$ | $\theta_5 - \theta_3$ | $\theta_6 - \theta_3$ |
|---|---|---|---|---|
| $\lvert\psi_{1i}\rvert$ | 9.462 | 8.588 | 8.951 | 8.079 |
| $\angle\psi_{1i}$ | $\angle-84.32°$ | $\angle-84.36°$ | $\angle-84.35°$ | $\angle-84.39°$ |

As seen from Tables I and II, the signals are grouped considering $\psi_{1i}$-s in same phase. However, for the group in Table I there is a large variation in $\lvert\psi_{1i}\rvert$-s, with signal $\theta_1 - \theta_3$ clearly an outlier. As expected from our deductions in Section III, this leads to poor denseness: $\kappa_1(\mathbf{Y}) = 0.975 > \kappa^*$. Therefore, when signal $\Delta(\theta_1 - \theta_3)$ is corrupted by injecting a signal component with negative damping, recovery is not guaranteed. As seen in Fig. 2 (a) the reconstructed signal traces the corruption.

In contrast, for the signal group in Table II, $\kappa_1(\mathbf{Y}) = 0.538 < \kappa^*$. This guarantees exact recovery of $\Delta(\theta_1 - \theta_3)$, as is evident from the plots in Fig. 2 (b). Also, the linear approximation derived in eqn. (16), $\frac{1}{\sqrt{n}}\left(1+\frac{\rho\sigma}{\mu}\right) = 0.553$ gives a reasonable estimate of $\kappa_1(\mathbf{Y})$ in guaranteeing recovery.
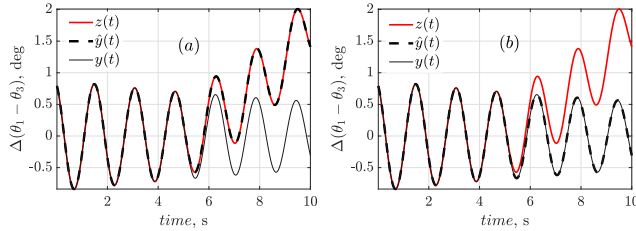


Fig. 2: Recovery of $\Delta(\theta_1 - \theta_3)$ for signal groupings in Tables I and II

### B. Case II: Grouping Signals from Field PMU Measurements

We consider detrended bus voltage magnitude signals $\lvert V_1\rvert$ to $\lvert V_{40}\rvert$, from 40 different PMU locations in New York Power Authority (NYPA). Denseness calculation on the entire data set yields $\kappa_1(\mathbf{Y}) = 0.549$, just enough to guarantee recovery of 1 in 40 signals. This ratio being abysmally low, our objective is to selectively group signals from this set using our proposed recommendations to improve corruption resilience.

We consider a 50 s window of archived data (assume previously recovered, and therefore, trusted) and perform spectral decomposition on each of the 40 signals. We observe two frequencies within the signal set− 0.25 Hz and 0.06 Hz. Next, with $\lvert V_1\rvert$ as reference we compute the output-to-output transfer function, and the relative modeshapes for all 40 signals at the mentioned frequencies− 0.25 Hz and 0.06 Hz, as described in [17]. Since the output-to-output transfer functions were computed with respect to a fixed reference, modeshapes thus obtained are equivalent to relative modal observabilities. Next, going by our propositions, we group signals having similar phase and magnitude of relative modal observabilities for *each* of the two frequency components. To do so, we use $k-$means clustering [18] on the signal set using the $2 \times 1$ feature vector of complex-valued relative observabilites.

TABLE III: SIGNAL SETS I AND II

| signal set I | $\lvert V_6\rvert$, $\lvert V_{15}\rvert$, $\lvert V_{19}\rvert$, $\lvert V_{20}\rvert$, $\lvert V_{21}\rvert$, $\lvert V_{26}\rvert$, $\lvert V_{27}\rvert$, $\lvert V_{28}\rvert$ |
|---|---|
| signal set II | $\lvert V_4\rvert$, $\lvert V_7\rvert$, $\lvert V_{11}\rvert$, $\lvert V_{13}\rvert$, $\lvert V_{16}\rvert$, $\lvert V_{17}\rvert$, $\lvert V_{22}\rvert$, $\lvert V_{24}\rvert$ |

Two such clusters− signal sets I and II, obtained for $k = 10$ are listed in Table III. Figures 3 (a) and 4 (a) show the time-domain plots of all 8 signals in each cluster, along with power spectral density (PSD) plots of one representative signal from each cluster in Figs 3 (b) and 4 (b). Clearly, signals in set I exhibit unimodal oscillations of 0.25 Hz, while those in set II indicate presence of both 0.25 Hz and 0.06 Hz oscillations.

TABLE IV: DENSENESS VALUES FOR SIGNAL SETS I AND II

| groups | $\kappa_1(\mathbf{Y})$ | $\kappa_1(\hat{\mathbf{\Psi}})$ | $\kappa_2(\mathbf{Y})$ | $\kappa_2(\hat{\mathbf{\Psi}})$ |
|---|---|---|---|---|
| signal set I | 0.3806 | 0.4109 | 0.5382 | 0.5530 |
| signal set II | 0.3752 | 0.3804 | 0.5275 | 0.5363 |

The denseness coefficients[1] $\kappa_1$ and $\kappa_2$ corresponding to $1-$sparse and $2-$sparse recoveries for these signal sets are listed in Table IV. It can be seen that for both the signal sets, $\kappa_2(\mathbf{Y}) < \kappa_2(\hat{\mathbf{\Psi}})$. This validates our claim in lemma 1. Further, in both cases, $\kappa_2(\hat{\mathbf{\Psi}}) < \kappa^*$, which guarantees exact recovery upto 2 of 8 signals in each group. This is a significant improvement from 1 in 40.
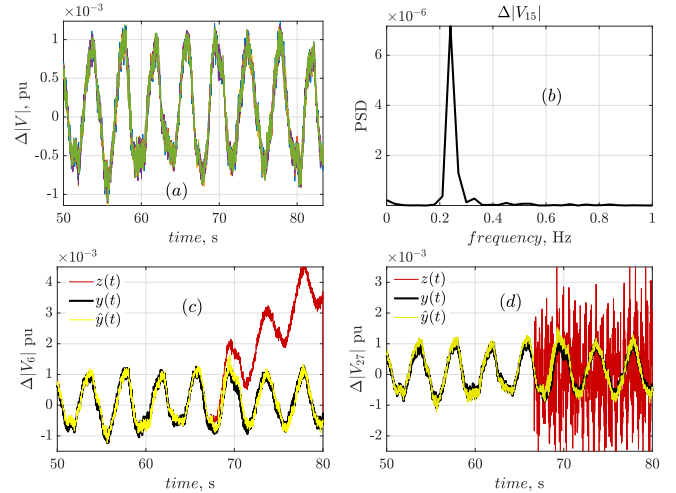


Fig. 3: Plots for (a) signal set I with (b) PSD, and (c)-(d) $2-$sparse recovery

Table V shows the denseness coefficients[2] of set II for each constituent frequency component, obtained corresponding to each complex-conjugate column pair $\hat{\mathbf{\Psi}}_\mathbf{j}$ of $\mathbf{\Psi} = \left[\hat{\mathbf{\Psi}}_\mathbf{1}\hat{\mathbf{\Psi}}_\mathbf{2}\right]$. As is seen, for each frequency component, the sufficiency

TABLE V: SET II: FREQUENCY-WISE DENSENESS[2] AND BOUNDS

| freq. | $\kappa_1(\hat{\mathbf{\Psi}}_\mathbf{i})$ | $\frac{1}{\sqrt{n}}\left(1+\frac{\rho_i\sigma_i}{\mu_i}\right)$ | $\kappa_2(\hat{\mathbf{\Psi}}_\mathbf{i})$ | $\sqrt{\frac{2}{n}}\left(1+\frac{\rho_i\sigma_i}{\mu_i}\right)$ |
|---|---|---|---|---|
| 0.25 Hz | 0.3794 | 0.3842 | 0.5259 | 0.5433 |
| 0.06 Hz | 0.3884 | 0.3953 | 0.5438 | 0.5590 |

[1] computed on singular vectors capturing 95% or more variance in data

[2] Ideally, $\kappa_s(\hat{\mathbf{\Psi}}) \geq \kappa_s(\hat{\mathbf{\Psi}}_\mathbf{j}) \, \forall \, j \leq k$, when computed on all $k$ singular vectors. Here, mode-wise variance minimization results in $1^{st}$ singular vector capturing 97% variance. $\kappa_s(\hat{\mathbf{\Psi}})$ thus computed, appears slightly less than some $\kappa_s(\hat{\mathbf{\Psi}}_\mathbf{j})$-s due to numerical approximations in truncation.

condition for 2−sparse recovery is attained. Moreover, it is seen that the bound on $\kappa_1$ derived in Section III, and extended to $\kappa_2$ using the identity $\kappa_s < \sqrt{s}\kappa_1$ [16], is sufficiently tight.
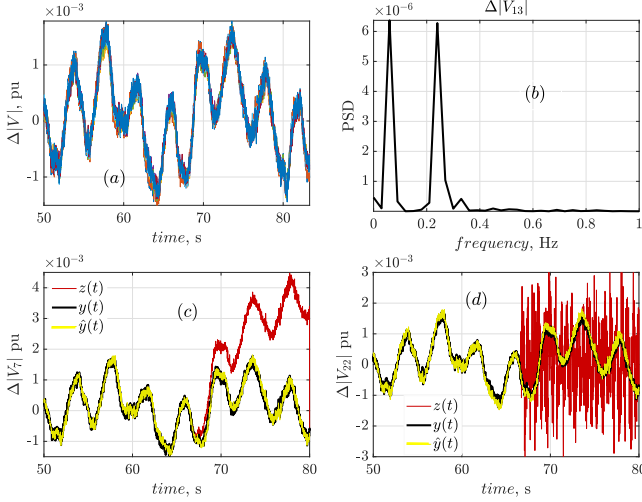


Fig. 4: Plots for (a) signal set II with (b) PSD, and (c)-(d) 2−sparse recovery

To validate our claim on resilience, we next corrupt signals $|V_6|$ and $|V_{27}|$ from set I, and $|V_7|$ and $|V_{22}|$ from set II. In signals $|V_6|$ and $|V_7|$, we inject an additive signal component with negative damping, while in signals $|V_{22}|$ and $|V_{27}|$ we replace the actual signal value with random spurious outliers. Corruption is introduced in 200 consecutive samples starting at $t = 68$ s, as shown in Figs 3 (c)-(d) and 4 (c)-(d). Recovery is performed independently for each set with subspace derived from its constituent signals. It can be observed that the recovery is exact as the reconstructed signal tracks the original.

Further, to underscore the importance of our propositions in grouping signals, we arbitrarily form signal set III taking 4 signals each from from sets I and II, as shown in Table VI. As before, we corrupt signals $|V_7|$ and $|V_{22}|$. For this group, the denseness values obtained are: $\kappa_1(\mathbf{Y}) = 0.709$ and $\kappa_2(\mathbf{Y}) = 0.995$, each of which is greater than $\kappa^*$. Therefore, recovery of signals is not guaranteed. This is evident from the erroneous reconstruction plots in Figs. 5 (a)-(b).
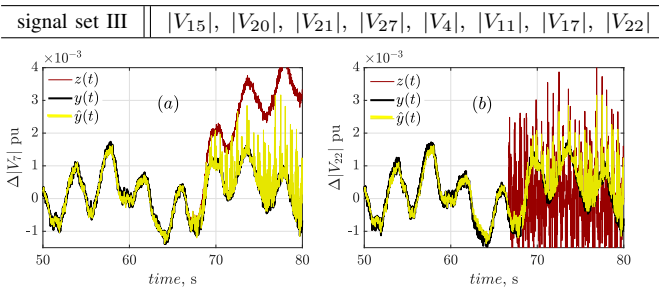
TABLE VI: SIGNAL SET III

| signal set III | $|V_{15}|$, $|V_{20}|$, $|V_{21}|$, $|V_{27}|$, $|V_4|$, $|V_{11}|$, $|V_{17}|$, $|V_{22}|$ |
|---|---|



Fig. 5: Incorrect recovery of 2 corrupted signals from signal set III.

## V. CONCLUSION

Insights were derived and recommendations were made for grouping signals to enhance denseness of a set – both considering availability of small-signal model, and in absence

thereof. It was shown that denseness of a set increased when signals were grouped with observabilities in same phase and variation in magnitudes minimized, for each poorly-damped mode. Further, it was shown that for a signal set sufficiently dense, the denseness coefficient increased linearly with increase in relative magnitude of the largest observability.

## REFERENCES

[1] V. Terzija, G. Valverde, D. Cai, P. Regulski, V. Madani, J. Fitch, S. Skok, M. M. Begovic, and A. Phadke, "Wide-Area Monitoring, Protection, and Control of Future Electric Power Networks," *Proceedings of the IEEE*, vol. 99, no. 1, pp. 80–93, Jan. 2011.

[2] F. Aminifar, M. Fotuhi-Firuzabad, A. Safdarian, A. Davoudi, and M. Shahidehpour, "Synchrophasor Measurement Technology in Power Systems: Panorama and State-of-the-Art," *IEEE Access*, vol. 2, pp. 1607–1628, 2014.

[3] K. Chatterjee, V. Padmini, and S. A. Khaparde, "Review of Cyber Attacks on Power System Operations," in *2017 IEEE Region 10 Symposium*, Jul. 2017, pp. 1–6.

[4] R. Bobba, E. Heine, H. Khurana, and T. Yardley, "Exploring a tiered architecture for NASPInet," in *2010 Innovative Smart Grid Technologies (ISGT)*, Jan. 2010, pp. 1–8.

[5] A. Ashok, M. Govindarasu, and J. Wang, "Cyber-Physical Attack-Resilient Wide-Area Monitoring, Protection, and Control for the Power Grid," *Proceedings of the IEEE*, vol. 105, no. 7, pp. 1389–1407, Jul. 2017.

[6] Y. Hao, M. Wang, J. H. Chow, E. Farantatos, and M. Patel, "Modelless Data Quality Improvement of Streaming Synchrophasor Measurements by Exploiting the Low-Rank Hankel Structure," *IEEE Trans. Power Syst.*, vol. 33, no. 6, pp. 6966–6977, Nov. 2018.

[7] P. Gao, R. Wang, M. Wang, and J. H. Chow, "Low-Rank Matrix Recovery From Noisy, Quantized, and Erroneous Measurements," *IEEE Trans. Signal Process.*, vol. 66, pp. 2918–2932, Jun. 2018.

[8] M. Liao, D. Shi, Z. Yu, Z. Yi, Z. Wang, and Y. Xiang, "An Alternating Direction Method of Multipliers Based Approach for PMU Data Recovery," *IEEE Trans. Smart Grid*, pp. 1–1, 2018.

[9] K. Mahapatra and N. R. Chaudhuri, "Malicious Corruption-Resilient Wide-Area Oscillation Monitoring Using Principal Component Pursuit," *IEEE Trans. on Smart Grid*, vol. 10, no. 2, pp. 1813–1825, 2019.

[10] ——, "Online Robust PCA for Malicious Attack-Resilience in Wide-Area Mode Metering Application," *IEEE Trans. Power Syst.*, pp. 1–1, 2019.

[11] T. T. Cai, L. Wang, and G. Xu, "New bounds for restricted isometry constants," *IEEE Transactions on Information Theory*, vol. 56, no. 9, pp. 4388–4394, Sep. 2010.

[12] P. Kundur, *Power System Stability and Control*. McGraw-Hill, Inc., 1994.

[13] E. J. Candes and M. B. Wakin, "An Introduction To Compressive Sampling," *IEEE Signal Processing Magazine*, vol. 25, no. 2, pp. 21–30, Mar. 2008.

[14] E. J. Candes and B. Recht, "Exact low-rank matrix completion via convex optimization," in *2008 46th Annual Allerton Conference on Communication, Control, and Computing*, Sep. 2008, pp. 806–812.

[15] E. J. Candes, "The Restricted Isometry Property and Its Implications for Compressed Sensing," *Comptes Rendus Mathematique*, vol. 346, no. 9, pp. 589–592, May 2008.

[16] C. Qiu, N. Vaswani, B. Lois, and L. Hogben, "Recursive Robust PCA or Recursive Sparse Recovery in Large but Structured Noise," *IEEE Transactions on Information Theory*, vol. 60, no. 8, pp. 5007–5039, Aug. 2014.

[17] D. J. Trudnowski, "Estimating Electromechanical Mode Shape From Synchrophasor Measurements," *IEEE Trans. on Power Syst.*, vol. 23, no. 3, pp. 1188–1195, 2008.

[18] S. Lloyd, "Least squares quantization in pcm," *IEEE Transactions on Information Theory*, vol. 28, no. 2, pp. 129–137, Mar. 1982.